



Contents lists available at SciVerse ScienceDirect

Deep-Sea Research II

journal homepage: www.elsevier.com/locate/dsr2

Bimodal distribution patterns of motile phytoplankton in relation to physical processes and stratification (Gulf of Finland, Baltic Sea)

Urmas Lips^{a,*}, Inga Lips^a

^a Marine Systems Institute, Tallinn University of Technology, Akadeemia tee 15a, 12618 Tallinn, Estonia

ARTICLE INFO

Keywords:

Motile phytoplankton
Dinoflagellates
Bimodal distribution
Thin layers
Vertical stratification
Gulf of Finland
Baltic Sea

ABSTRACT

The dynamics and vertical distribution patterns of chlorophyll *a* and motile phytoplankton species in relation to the vertical stratification and its spatial and temporal variations were analyzed on the basis of observational data collected in the Gulf of Finland in July 2010. Bimodal vertical distribution of phytoplankton characterized by a thick maximum in the upper 10 m layer and a thin maximum in the deeper part of the thermocline, where the chlorophyll *a* fluorescence values often exceeded those in the upper layer, was observed in the areas of locally weaker stratification at the mesoscale in the second half of July. We suggest that the observed bimodal distribution pattern was a result of the downward migration of phytoplankton through the thermocline at night and asynchronous upward movement of cells with a migration cycle longer than 24 h. The main species found in the sub-surface maxima were the dinoflagellates *Heterocapsa triquetra* and occasionally *Dinophysis acuminata*. Biomass of *H. triquetra* increased in the surface layer concurrently with the appearance of sub-surface biomass maxima under conditions of relatively high horizontal variability of vertical stratification at the mesoscale. It supports our suggestion that the mesoscale dynamics favors successful vertical migration of this species between the surface layer and deep nitrate reserves. Sub-surface maxima of phytoplankton biomass, as well as vertical migration, leading to selective transport of nutrients, have to be taken into account in the regional ecosystem models, both to forecast phytoplankton blooms and describe more precisely the seasonal dynamics of nutrients and phytoplankton primary production in the stratified estuaries.

© 2013 Elsevier Ltd. All rights reserved.

1. Introduction

Vertical migration is widely acknowledged as an effective survival strategy for flagellated phytoplankton in stratified environments where the main resources—light and nutrients—are separated by physical gradients. In the case of shallow pycnoclines, cells are able to perform diel vertical migration aggregating near the sea surface during the day and in the pycnocline or near the seabed at night (Hall and Paerl, 2011; Sullivan et al., 2010). In estuaries where the euphotic depth and nitracline depth are well separated in summer, bimodal vertical distribution patterns have been often observed (Lips et al., 2010; Townsend et al., 2005).

It is suggested that the bimodal distribution of motile phytoplankton is a result of asynchronous vertical migration of cells between the euphotic upper layer and nutrient reserves below the pycnocline (Ralston et al., 2007). On the other hand, often, when bimodal distribution has been observed, the sub-surface maximum could be regarded as a thin phytoplankton layer according to the most recognized definition (Deksheniaks et al., 2001).

Several physical processes, such as straining by shear, intrusion, and gyrotactic trapping, and biological processes including convergent swimming and *in situ* growth have been suggested as mechanisms of thin-layer formation and persistence (see an overview by Durham and Stocker, 2012). Recent studies in the field (Sullivan et al., 2010; Velo-Suarez et al., 2010) and in the mesocosms (Jephson et al., 2011) suggest that physical processes and stratification, as well as species-specific biological behavior, are crucial for the formation of biomass maxima below the pycnocline.

A number of studies have reported the occurrence of sub-surface or deep maxima of phytoplankton biomass in the Baltic Sea (Hällfors et al., 2011; Kononen et al., 2003; Gisselson et al., 2002). The main species forming such biomass maxima belong to dinoflagellates, *i.e.*, *Dinophysis acuminata* and *D. norvegica* Claparède and Lachmann 1859, found mostly in the Baltic Proper and the western Gulf of Finland (Hällfors et al., 2011), and *Heterocapsa triquetra* (Ehrenberg) Stein in the Gulf of Finland (Kononen et al., 2003). Kononen et al. (2003) suggested that the surface bloom of *H. triquetra* in the Gulf of Finland in summer 1998 was formed on the basis of a nitrate pool utilized by migrating cells below the thermocline. While the sub-surface biomass maxima and nocturnal, synchronous downward migration of *H. triquetra* was

* Corresponding author. Tel.: +372 6204304; fax: +372 6204301.
E-mail address: urmas.lips@msi.ttu.ee (U. Lips).

observed in July 2009 (Lips et al., 2011), the upward migration was not documented at the same site. It could be suggested that upward migration was asynchronous or took place at some other geographical locations.

The Gulf of Finland is a stratified estuary where nutrient-depleted surface waters are separated from the nutrient-rich deeper layers by the seasonal thermocline in summer. High values of kinetic energy of mesoscale fluctuations have been reported on the background of general cyclonic circulation (Laanemets et al., 2011; Alenius et al., 1998). In accordance with this, mesoscale patterns in horizontal distribution of phytoplankton in the surface layer of the Gulf of Finland are frequently observed, both in the field (Lips and Lips, 2010; Kononen et al., 1996) and using remote-sensing methods (Kahru et al., 2007). We hypothesize that the motile phytoplankton species benefit from the existing mesoscale circulation patterns in this stratified estuary. Since different species can form the sub-surface biomass maxima, the analysis of links between the mesoscale physical processes and phytoplankton dynamics should be species-specific and incorporate biological/ecological processes, such as migration behavior, mixotrophy, and the ability to utilize certain nutrient sources, such as organic nitrogen compounds in the thermocline or nitrate below it. Information on species forming sub-surface biomass maxima and their survival strategies is particularly important due to the fact that among them some are potentially toxic (Setälä et al., 2011) or can form harmful blooms (Lindholm and Nummelin, 1999).

The main aim of the present paper is to demonstrate the links between the physical processes and characteristics of bimodal vertical distribution of summer phytoplankton in the stratified Gulf of Finland. We focus our analysis on the dynamics and vertical distribution patterns of chlorophyll *a* and motile phytoplankton species in relation to the horizontal variability of vertical stratification at the mesoscale.

2. Material and methods

The data set analyzed in the present study was collected in summer 2010 in the Gulf of Finland, Baltic Sea (see map in Fig. 1A) by observations and sampling aboard a research vessel and a ferry traveling between Tallinn and Helsinki, autonomous measurements at a buoy station, and towed undulating-vehicle (Scanfish) surveys. Vertical profiles of temperature, salinity, and chlorophyll *a*

(Chl *a*) were acquired weekly (or more frequently) at station AP5 from 30 June to 2 August using an OS320*plus* CTD probe (Idronaut S.r.l.) equipped with a Seapoint Chl *a* fluorometer. Water samples were collected with a vertical resolution of 5–10 m for analyses of inorganic nutrient (PO_4^{3-} and $\text{NO}_2^- + \text{NO}_3^-$) concentrations, Chl *a* content, and phytoplankton species composition and biomass.

The Ferrybox system (-4H- Jena Engineering GmbH) aboard the passenger ferry "Baltic Princess" (AS Tallink Grupp) recorded temperature, salinity, and Chl *a* fluorescence in the surface layer (water intake was approximately at 4 m depth) twice a day along the ferry route (Fig. 1A). Time resolution of measurements was 20 s corresponding approximately to a spatial resolution of 150 m. Water sampling upto 17 locations along the ferry route was conducted on 30 June, 5 July, 12 July, 18 July, 25 July, and 1 August. The water samples were analyzed for the same parameters as those collected by the research vessel.

The autonomous profiler (Idronaut S.r.l.; surface buoy designed by Flydog Solutions Ltd.) was deployed at station AP5 (Fig. 1A) from 30 June to 4 August. Vertical profiles of temperature, salinity, and Chl *a* fluorescence in the water layer from 2 to 45 m were acquired with a time resolution of 3 h and a vertical resolution of 10 cm. Measurements were conducted using an OS316*plus* CTD probe (Idronaut S.r.l.) equipped with a Seapoint Chl *a* fluorometer.

Surveys using a towed undulating vehicle (Scanfish) equipped with conductivity, temperature, pressure (Neil Brown Mark III), and Chl *a* fluorescence (Trios microFlu-chl-A, sampling rate 5 Hz) sensors were conducted to map the horizontal distribution of phytoplankton Chl *a* in the water column from 2 to 45 m. Data from the surveys on 20–21 July, 22 July, 26 July, 27 July, 30 July, and 2 August are used in the present analysis (see configuration of surveys in Fig. 1B). Before the surveys on 22 July and 2 August, the same cross-section was sampled at 13 stations (Fig. 1A) for CTD profiles and nutrient, Chl *a*, and phytoplankton species composition analyses from discrete samples. Vertical resolution of water sampling was 5 m, however, the sub-surface Chl *a* maxima were sampled at the depths of observed fluorescence peaks. All measurements were conducted mostly in the daytime with the exception of the polygon-like survey by Scanfish at night on 20–21 July.

The samples for nutrient analyses were deep-frozen after collection and analyzed at the on-shore laboratory using the automatic nutrient analyzer Lachat QuikChem 8500 Series 2 (Lachat Instruments, Hach Company). Nutrient analyses were carried out according to the recommendations of USEPA, ISO and

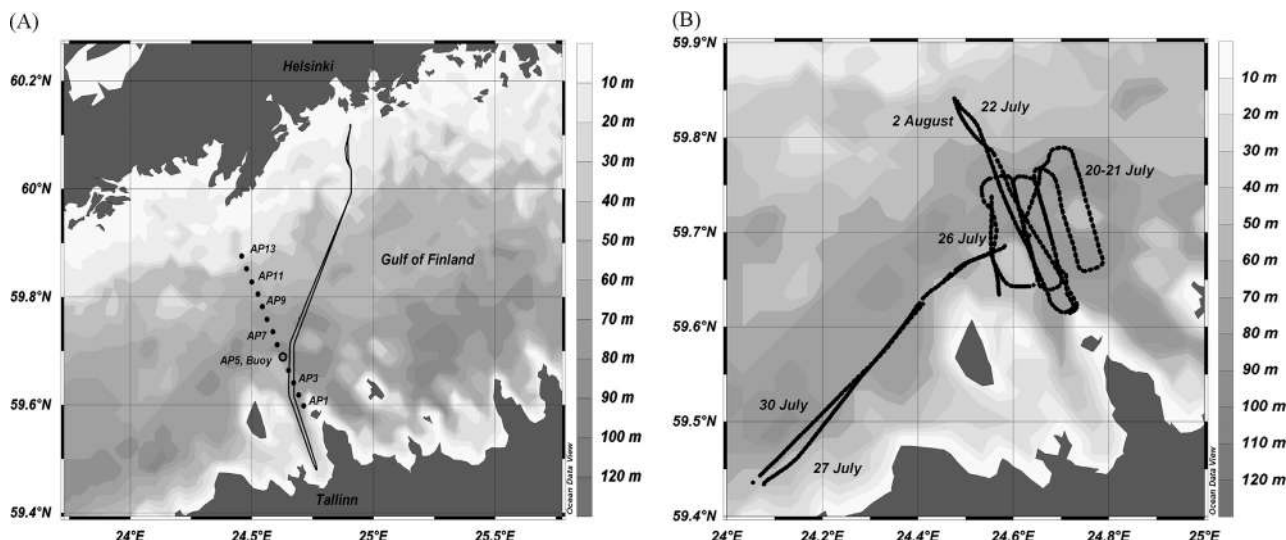


Fig. 1. Map of the study area where (A) locations of the sampling section AP1–AP13, buoy station (open circle), and ferry route Tallinn–Helsinki, and (B) towed undulating vehicle surveys are indicated.

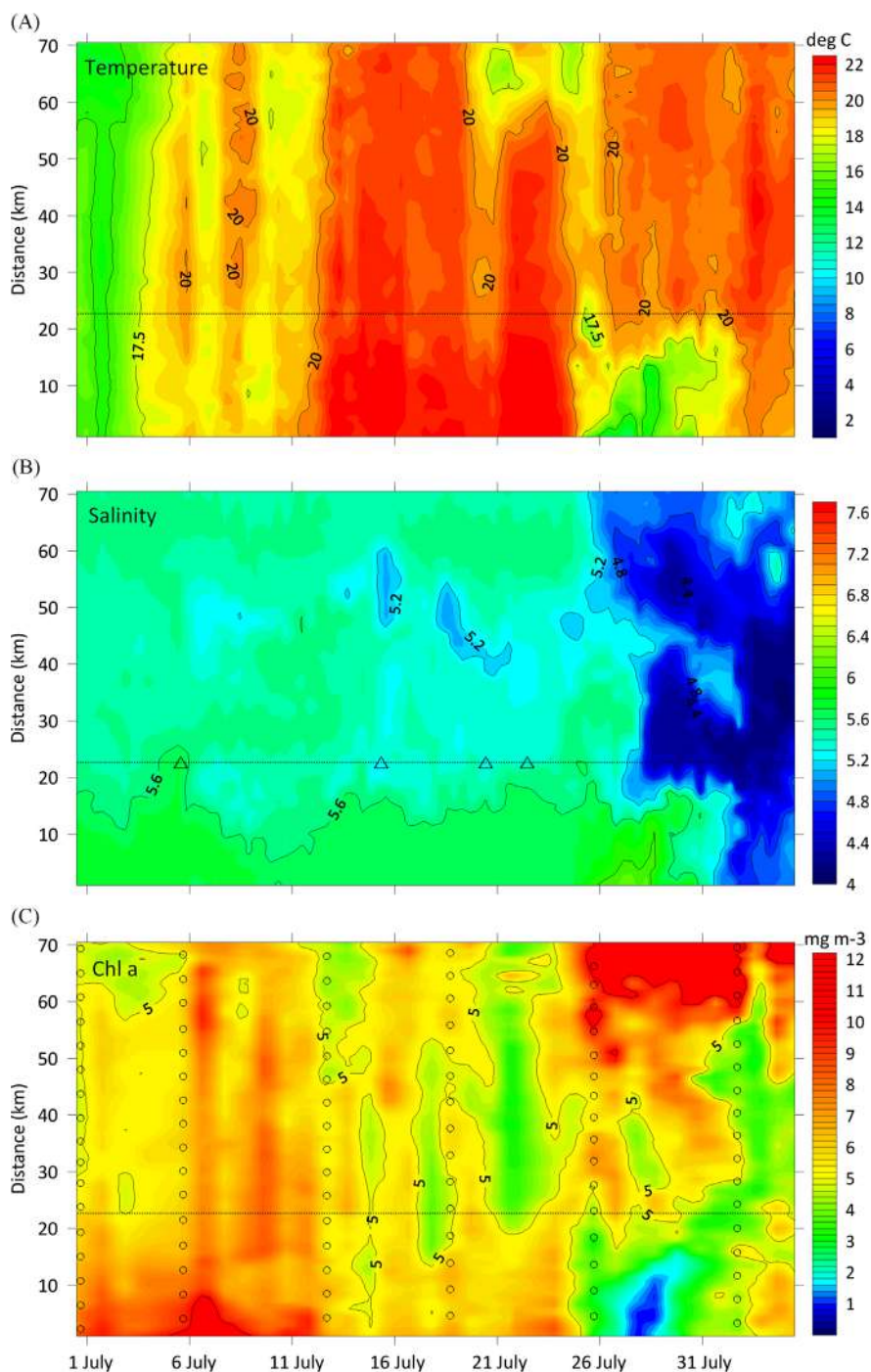


Fig. 2. Temporal variations of horizontal distribution of (A) temperature ($^{\circ}\text{C}$), (B) salinity, and (C) chlorophyll *a* (mg m^{-3}) along the ferry route Tallinn–Helsinki from 30 June to 4 August 2010. On the y-axis the distance from Tallinn Bay is given. Open circles show the Ferrybox sampling sites (lower panel), horizontal dotted line indicates the location of the buoy station (data presented in Fig. 3), and triangles mark the sampling dates at station AP5 (middle panel; data presented in Fig. 5).

DIN standards, methods 31-107-04-1-D NO_3 (Egan, 2000) and 31-115-01-1-I PO_4 (Ammerman, 2001). The lower detection range for PO_4^{3-} and $\text{NO}_2^- + \text{NO}_3^-$ were 0.008 and 0.014 μM , respectively.

Chl *a* concentration in the water samples was determined on Whatman GF/F glass-fiber filters following extraction at room temperature in the dark with 96% ethanol for 24 h. Chl *a* content from the extract was measured spectrophotometrically (Thermo Helios γ) in the laboratory (HELCOM, 1988). Phytoplankton subsamples (100 ml) were preserved with acid Lugol solution and analyzed using the Utermöhl (1958) technique and PhytoWin software by Kahma Ky. All biomass data are given in wet weight concentrations (Olenina et al., 2006).

Chl *a* fluorescence measured aboard the research vessel and at the buoy station (Seapoint sensors) was calibrated against Chl *a* measured in the water samples collected from 9 June to 2 August. The following equation of the regression line found between the measured Chl *a* and fluorescence values was used to convert fluorescence into Chl *a* in mg m^{-3} : $\text{Chl } a = 2.47 \times F$ ($r^2 = 0.41$, $n = 50$ data pairs, where F is the fluorescence measured by the Seapoint sensor). By comparing the Chl *a* values at the CTD stations with the Chl *a* fluorescence values recorded by Scanfish (Trios sensor) along the same section on 22 July, a conversion factor of 0.91 was found to convert Scanfish fluorescence into Chl *a* in mg m^{-3} . Chl *a* fluorescence measured by the Ferrybox system was calibrated against Chl *a* measured in the laboratory from

the water samples collected at 17 sampling sites on 12, 18, and 25 July and 1 August. The following equation of the regression line was used to convert fluorescence values into Chl *a* in mg m^{-3} : $\text{Chl } a = 2.34 \times F - 2.41$ ($r^2 = 0.77$, $n = 66$ data pairs, where F is the fluorescence measured by SCUFA (Turner Designs) attached to the Ferrybox system).

3. Calculations

Observations in the Gulf of Finland have revealed the occurrence of sub-surface Chl *a* maxima layers in the deeper part of the thermocline coinciding with the nitracline depth (Lips et al., 2010;

Kononen et al., 2003). On the basis of vertical profiles collected at a single location with a high temporal resolution in July 2009, a link between the nocturnal downward migration of phytoplankton and formation of sub-surface maxima was suggested (Lips et al., 2011). Occurrence and horizontal patchiness in intensities of sub-surface maxima have been related to the mesoscale hydrodynamic processes (Lips et al., 2010; Velo-Suarez et al., 2010) and vertical stratification (Lips et al., 2011). Mesoscale eddies cause vertical displacement of isopycnals and mixing (Reissmann et al., 2009) as well as clear spatial variations in vertical stratification—central parts of anti-cyclonic eddies are characterized by weaker and cyclonic eddies by stronger stratification. Jephson et al. (2011) showed in their laboratory experiment that *H. triquetra* was able to

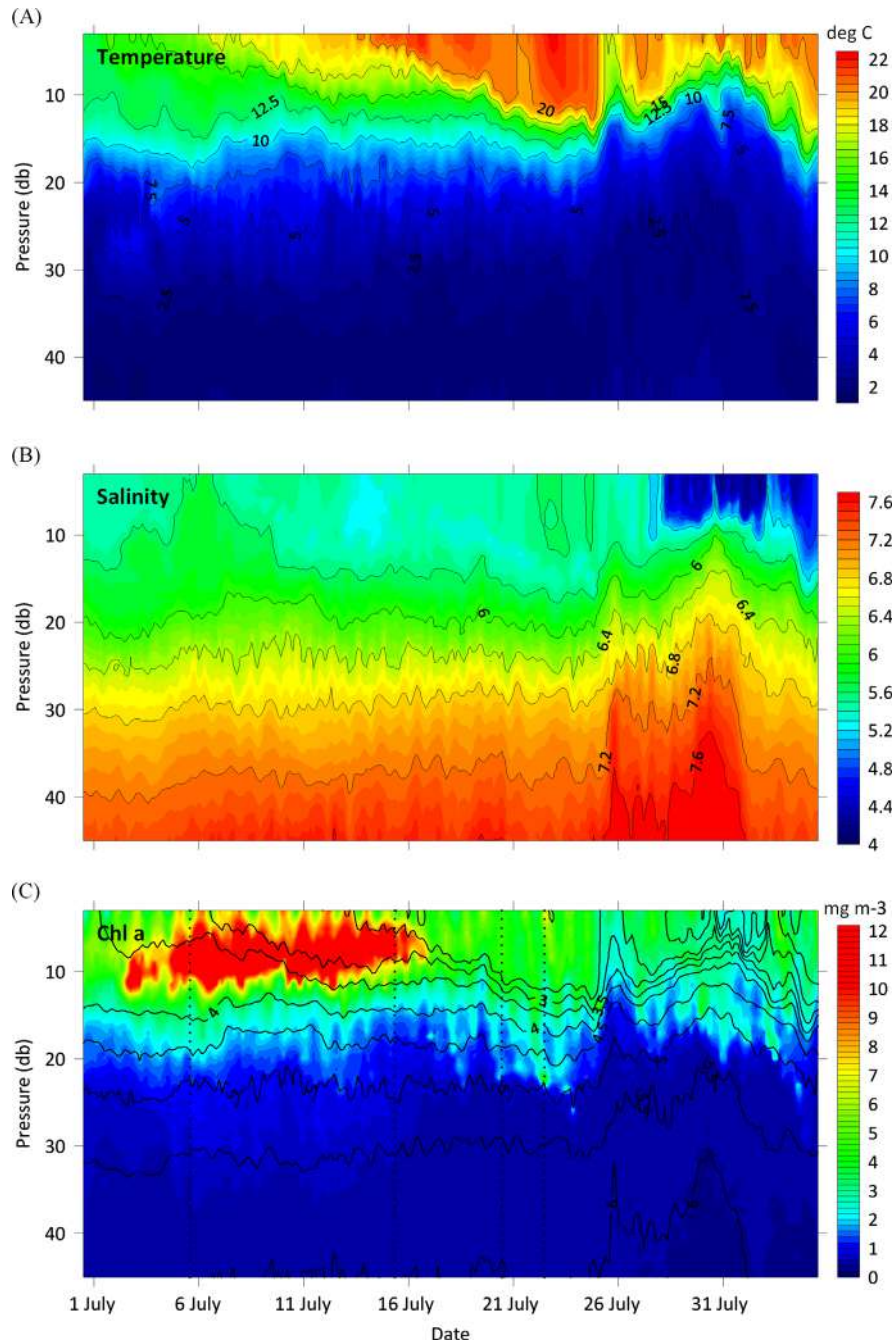


Fig. 3. Temporal variations of vertical distribution of (A) temperature ($^{\circ}\text{C}$), (B) salinity, and (C) chlorophyll *a* (mg m^{-3} ; color scale) and density anomaly (black lines, kg m^{-3}) at the buoy station in the Gulf of Finland (see location in Fig. 1) from 30 June to 4 August 2010. Dotted lines in the lower panel indicate the sampling dates and time at station AP5 close to the buoy station (data presented in Fig. 5).

migrate through a moderate salinity gradient but accumulated at the pycnocline in the case of a very strong vertical gradient of salinity. In order to link the occurrence of sub-surface maxima of phytoplankton biomass with the vertical stratification, we have analyzed the collected Chl *a* fluorescence profiles collected in the Gulf of Finland in July 2010 for local maxima and calculated a stratification parameter using corresponding density anomaly profiles as described below.

The Chl *a* fluorescence data collected with a sampling rate of 5 Hz when the Scanfish was moving up or down with a speed of 0.6 m s^{-1} were preprocessed and stored with a vertical resolution of 20 cm. A local maximum was taken into account if the difference between the Chl *a* values in this local maximum and a local minimum above it exceeded 0.5 mg m^{-3} . The sub-surface maximum was determined if a local Chl *a* maximum occurred at a depth deeper than 12 m, which is approximately equal to the euphotic depth in the Gulf of Finland in summer (Lips et al., 2010). When presenting statistical characteristics, a sub-set of detected maxima was selected with the maximum Chl *a* value $> 4.5 \text{ mg m}^{-3}$. This value corresponds to a criterion of thin phytoplankton layers stating that the Chl *a* fluorescence level should exceed the background value by at least three times (background Chl *a* level in our study was from 1 to 1.5 mg m^{-3} in the sub-surface layer).

Vertical stratification was described on the basis of corresponding vertical profiles of density by calculating a stratification parameter using an equation similar to that introduced to estimate the potential energy anomaly P (Simpson et al., 1990)

$$P = \frac{1}{h_2 - h_1} \int_{-h_2}^{-h_1} (\rho_A - \rho(z)) g z \, dz, \quad \rho_A = \frac{1}{h_2 - h_1} \int_{-h_2}^{-h_1} \rho(z) \, dz$$

where $\rho(z)$ is the density profile in the water layer between the depths h_1 and h_2 . The stratification parameter P (J m^{-3}) is the work required to bring about complete mixing of the water column under consideration. In the present study, the stratification parameter was estimated in the water layer between $h_1 = 3 \text{ m}$ and $h_2 = 25 \text{ m}$. The shallower limit was chosen to guarantee that most of the profiles could be taken into account (Scanfish has reached this depth before turning downward), and the deeper limit was

taken just below the average depth of Chl *a* maxima observed during the study period.

4. Results

4.1. Background

According to the variations in the spatial distribution of temperature and salinity along the ferry route Tallinn–Helsinki (Fig. 2A and B) and at the buoy station (Fig. 3A and B), the study period from 30 June to 4 August 2010 can be divided into two clearly different phases. The first half of July was characterized by a gradual increase in surface water temperature. Due to the surface heating, the vertical gradient through the seasonal thermocline also increased. Horizontal variability of both temperature and salinity in the surface layer was relatively low.

In contrast, high spatial and temporal variability of temperature and salinity was observed in the second half of July. A moderate coastal upwelling event appeared near the northern coast from 20 to 24 July followed by a pronounced upwelling event near the southern coast from 25 July to 1 August (Fig. 2A). In association with the second upwelling event, low salinity waters were transported in the surface layer from the east into the study area. One of those low-salinity water branches appeared along the upwelling front, which was surfacing close to the buoy station (Fig. 2B). Vertical stratification was also very variable in the second half of July (Fig. 3A and B). First, a gradual deepening of the thermocline was observed at the buoy station from 17 to 24 July. After that, rapid alterations in temperature and salinity distribution occurred, which were caused by the upwelling development and movement of low salinity waters into the study site. Vertical salinity distribution in the sub-surface layer was also significantly influenced by the second upwelling event, resulting in a rapid upward movement of isohalines on 25 July (Fig. 3B).

During the first 12 days of July, the Chl *a* concentrations in the surface layer were mostly higher in the southern part than those in the central and northern parts of the gulf (Fig. 2C). After a period of relatively uniform horizontal distribution of Chl *a* from 12 to 24 July, the concentrations decreased in the upwelling area near the southern coast and remarkably increased near the northern coast of the Gulf of Finland on 25 July, where the highest Chl *a*

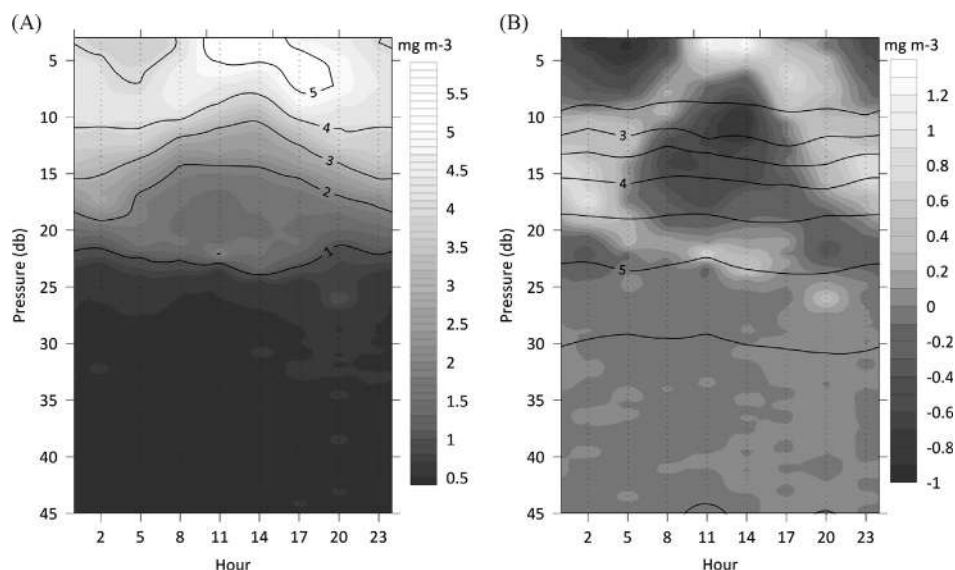


Fig. 4. Average daily variation of (A) vertical distribution of chlorophyll *a* (mg m^{-3}) and (B) chlorophyll *a* deviations from the daily average value at each depth (mg m^{-3}) at the buoy station (see location in Fig. 1) in the period from 17 to 24 July 2010.

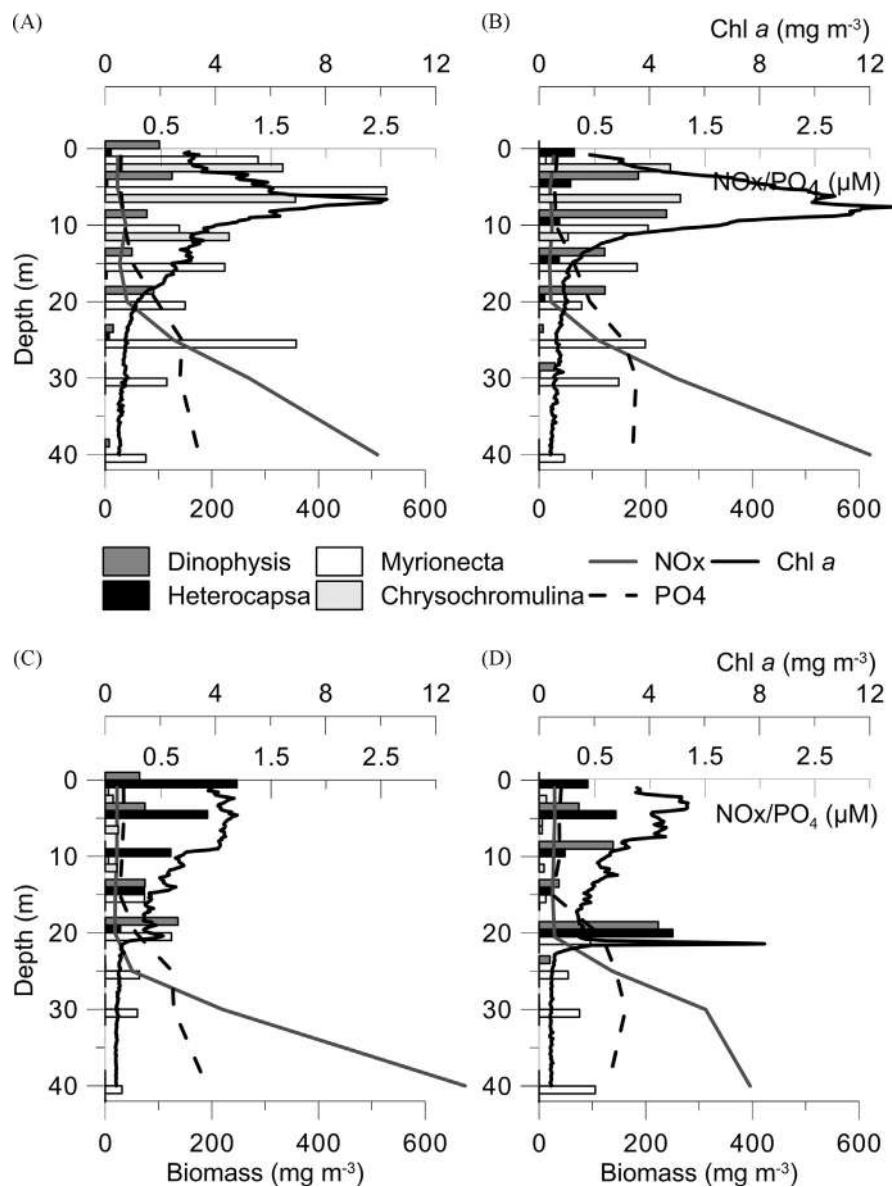


Fig. 5. Vertical profiles of chlorophyll *a*, phosphates, nitrates+nitrites (NO_x), and biomass of selected species at station AP5 on (A) 5 July (05.07.10. at 14:00), (B) 15 July (15.07.10. at 8:00), (C) 20 July (20.07.10. at 10:30), and (D) 22 July 2010 (22.07.10. at 11:20).

concentrations for the entire study period were retained until 1 August.

Two distinct patterns of vertical distribution of Chl *a* at the buoy station were revealed (Fig. 3C). The highest Chl *a* concentrations were mainly recorded in the water layer from 3 to 13 m in the first half of July, most probably reflecting the presence/dominance of *Chrysochromulina* species (see the next section). A minimum in the diel cycle of Chl *a* fluorescence in the near-surface layer at noon in this period can be attributed to the fluorescence quenching effect. In the second half of the study period, in contrast, a maximum in the diel cycle of Chl *a* fluorescence was observed in the surface layer at noon (Fig. 3C). This pattern is also seen in the average daily variations of vertical Chl *a* distribution constructed for the period 17–24 July (Fig. 4A). Chl *a* maximum revealed a vertical diel excursion from the near-surface layer at noon to 10 m depth at night. In addition, the sub-surface Chl *a* maxima observed occasionally at the deeper part of the thermocline within this period (and later; see Fig. 3C) are also visible in the daily average Chl *a* distribution plot. An average time-depth map of temporal variations of Chl *a* deviations from

the daily average at the certain depth illustrates the described dynamics (Fig. 4B).

The nutrient conditions did not change remarkably during the study period at the buoy station site (station AP5; see Fig. 5A–D). Both phosphate and nitrate–nitrite concentrations were close to or below the detection limit in the surface layer. The phosphacline had a shallower position and was situated between the sampling depths of 15 and 20 m while the nitracline was situated between 20 and 25 m. Based on the results of sampling aboard the research vessel in the second half of July, we can conclude that in the case of the characteristic bimodal Chl *a* distributions, the sharp sub-surface Chl *a* maximum almost always coincided with the nitracline (Figs. 5D and 6).

4.2. Phytoplankton species dynamics

According to the Ferrybox sampling from 30 June to 18 July, the community in the surface layer between Tallinn and Helsinki was dominated by prymnesiophyte *Chrysochromulina* spp. Lackey and cyanobacteria *Aphanizomenon* sp. (L.) Ralfs together with

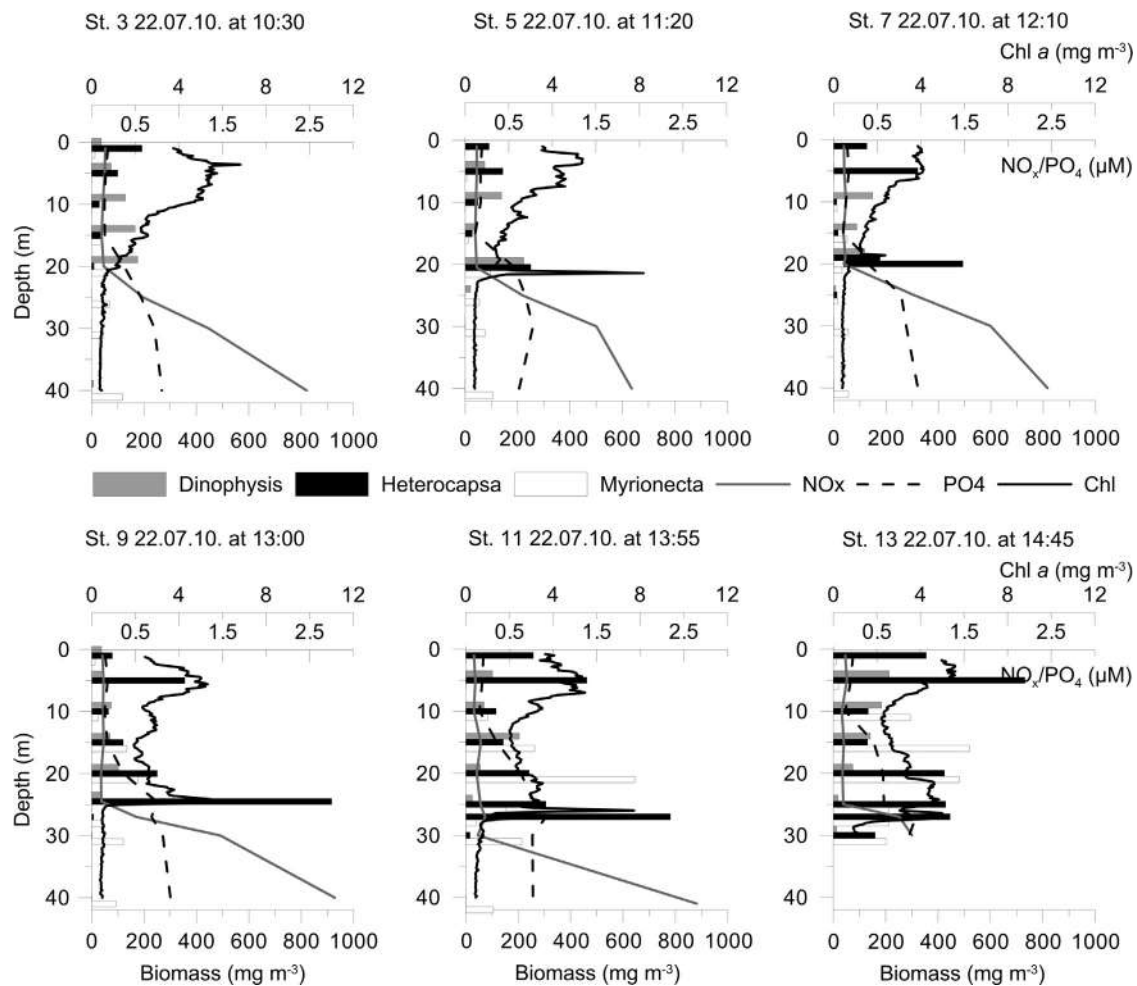


Fig. 6. Vertical profiles of chlorophyll *a*, phosphates, nitrates+nitrites (NO_x), and biomass of selected species at stations AP3, AP5, AP7, AP9, AP11, and AP13 on 22 July 2010.

Anabaena (Bory) spp. *Chrysochromulina* spp. were especially dominant on 5 July in the southern half of the gulf where they formed 28–76% of total wet weight biomass. Dinoflagellate *H. triquetra* biomass increased in the northern half of the cross-section in the second half of July and this species became the most dominant at a few northernmost sampling sites on 25 July. Maximum wet weight biomass values of *H. triquetra* of 890 mg m⁻³ and 990 mg m⁻³ were observed in the surface layer on 25 July and 1 August, respectively.

Sampling close to the buoy station (AP5) confirmed that the upper 10 m layer had a very high contribution of *Chrysochromulina* species (app. 40% with abundances of 4–6.5 million cells l⁻¹) in the beginning of July (Fig. 5A). The biomass of photosynthetic ciliate *Myrionecta rubra* (Lohmann 1908) Jankowski 1976 was also high at both 5 m and 25 m depth. By mid-July, the contribution of *Chrysochromulina* spp. had decreased down to 10–14% of total wet weight biomass in the upper 5 m layer and *M. rubra* was found mostly below 10 m depth (Fig. 5B). The dinoflagellate *D. acuminata* had high biomass and abundance values (6000–13000 cells l⁻¹) from 5 m depth down to 20 m depth (Fig. 5B). On 20–22 July, the upper 10 m layer was dominated by filamentous cyanobacteria (upto 70–80% of total wet weight biomass; data not shown). The dinoflagellate *H. triquetra* was mostly found in the upper mixed layer and there was a moderate *D. acuminata* and *M. rubra* biomass maximum at 20 m depth on 20 July (Fig. 5C). During the next sampling on 22 July, a sub-surface maximum of *D. acuminata* and *H. triquetra* was observed at 20.5 m depth just above the nitracline

while moderate biomass of both species was found in the upper 10 m layer (Fig. 5D).

The highest number of thin sub-surface maxima of phytoplankton biomass was found during the cross-gulf sampling (see location in Fig. 1) on 22 July. Thirteen stations were sampled using CTD and rosette sampler from 9:30 a.m. to 2:40 p.m. and high-resolution mapping was conducted using a towed undulating vehicle from 3:10 to 5:40 p.m. Vertical distribution of migrating species is described on the basis of phytoplankton samples collected at every second station from AP3–AP13 (Fig. 6; see the location of stations in Figs. 1 and 7C). The sub-surface maxima of the dinoflagellate *H. triquetra* were observed just above the nitracline at almost all sampled stations with a clearly higher biomass of this species in the northern half of the cross-section. However, within this high biomass section with a clear bimodal Chl *a* distribution pattern, the opposite horizontal gradients of *H. triquetra* biomass were observed in the surface and sub-surface layer. The highest sub-surface biomass of *H. triquetra* (916 mg m⁻³) was registered in the thin Chl *a* maximum layer at 25 m depth at station AP9, while at the northernmost stations AP11 and AP13 it was 781 mg m⁻³ and 446 mg m⁻³, respectively. In the surface layer (at 5 m depth), the *H. triquetra* biomass increased from 355 mg m⁻³ at station AP9 to 732 mg m⁻³ at station AP13. The local minimum between the two maxima in the bimodal vertical Chl *a* and biomass distributions was much less pronounced at the northernmost stations AP11 and AP13.

The photosynthetic ciliate *M. rubra* had significantly higher biomass values at all depths below 10 m at the northern part of the

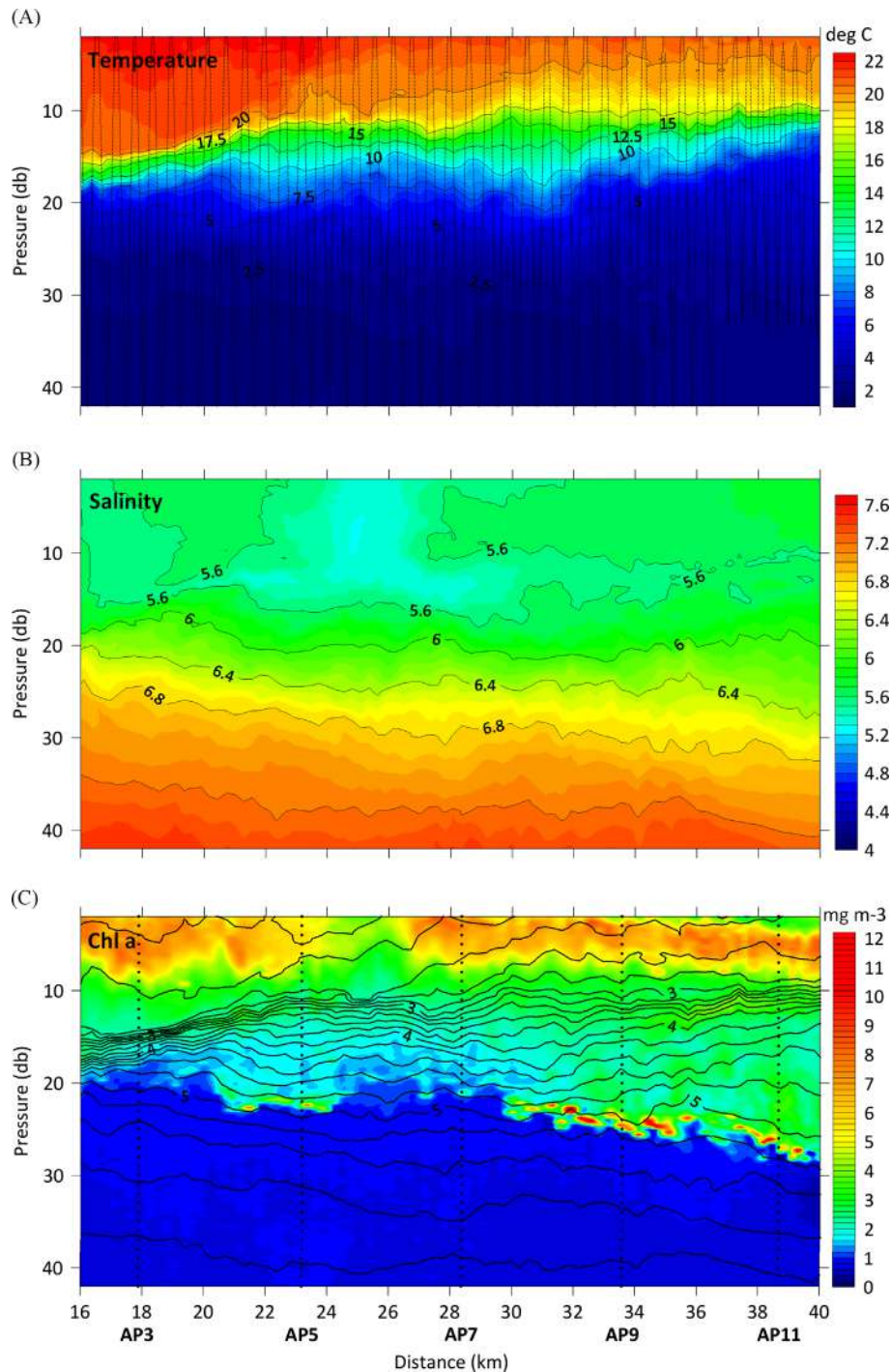


Fig. 7. Vertical sections of (A) temperature ($^{\circ}\text{C}$), (B) salinity, and (C) chlorophyll *a* (mg m^{-3} ; color scale) and density anomaly (kg m^{-3} , black lines) measured by the towed undulating vehicle (Scansfish) on 22 July 2010. The Scansfish trajectory is shown in the upper panel as dotted lines. Distance on the x-axis is calculated from the same point in Tallinn Bay as for the Ferrybox route (Fig. 2, y-axis). Locations of stations AP3, AP5, AP7, AP9, and AP11 are indicated as dotted lines in the lower panel (data presented in Fig. 6).

cross-section compared with the stations at the southern half of the cross-section. At all sampled stations, the moderate *D. acuminata* biomass was detected mostly at depths below 5 m. On the basis of abundance values, the *M. rubra* maxima were found at the 20 m depth, except station AP13, where the *M. rubra* maximum abundance was at 10 m depth ($> 107,000$ cells l^{-1}). The size distribution of *M. rubra* was also different in this sample from all other sampled stations: very small cells (size class 10–15 μm) were dominating ($> 73,000$ cells l^{-1}). At the same time, the size distribution of *H. triquetra* cells in the surface and sub-surface

layer did not differ significantly along the entire sampled transect. The dominant size classes were 22–24 μm and 25–28 μm with relative proportions of 60% and 40%, respectively.

4.3. Sub-surface maxima, thin layers and stratification

Altogether 359 sub-surface Chl *a* maxima were detected on the recorded 807 vertical profiles, among them 160 maxima with Chl *a* content > 4.5 mg m^{-3} (Table 1). Geographically, the sub-surface maxima were not restricted to a specific area of the gulf—they

Table 1

The number of observed sub-surface Chl *a* fluorescence maxima—the numbers for maxima with Chl *a* > 4.5 mg m⁻³ and in total are given. Average ± standard deviation of Chl *a*, pressure, temperature, salinity, and sigma-*t* in Chl *a* maxima > 4.5 mg m⁻³. Stratification parameter estimated between the depths 3 and 25 m for all profiles and for profiles containing sub-surface maxima.

Date	Number of maxima > 4.5 mg m ⁻³ and in total/number of profiles	Chl <i>a</i> fluorescence maximum (median/75th percentile) (mg m ⁻³)	Pressure (average ± stdev) (db)	Temperature (average ± stdev) (°C)	Salinity (average ± stdev) (kg m ⁻³)	Sigma- <i>t</i> (average ± stdev) (J m ⁻³)	Stratification parameter (average ± stdev; all) (J m ⁻³)	Stratification parameter (average ± stdev; max) (J m ⁻³)
20–21 July	57/94/246	5.94/8.43	17.8 ± 2.1	8.03 ± 3.23	5.91 ± 0.23	4.44 ± 0.54	70.3 ± 4.4	69.1 ± 6.4
22 July	42/55/94	10.04/13.04	24.4 ± 1.8	3.95 ± 0.86	6.34 ± 0.11	5.03 ± 0.11	67.9 ± 9.2	60.6 ± 5.1
26 July	0/35/137	–	–	–	–	–	67.2 ± 6.3	–
27 July	32/88/124	6.73/8.65	18.5 ± 1.7	4.18 ± 0.80	6.79 ± 0.04	5.39 ± 0.04	56.4 ± 14.0	51.0 ± 6.5
30 July	25/58/116	6.06/6.71	20.8 ± 2.4	3.20 ± 0.56	6.86 ± 0.08	5.46 ± 0.07	65.1 ± 14.6	71.6 ± 6.3
2 August	4/9/90	6.47/7.29	20.8 ± 0.5	6.17 ± 0.92	5.78 ± 0.07	4.51 ± 0.02	75.2 ± 7.0	68.9 ± 1.9
Total	160/359/807	6.58/9.81	20.2 ± 3.4	5.39 ± 2.86	6.34 ± 0.42	4.95 ± 0.54	67.2 ± 10.9	63.4 ± 9.6

were observed during different surveys in the central part, near the northern slope, and near the southern slope. The highest proportion of profiles with intense sub-surface maxima—i.e., equal to the highest proportion of bimodal Chl *a* profiles—was observed at the gulf's cross-section on 22 July (Table 1 and Fig. 7). The average values of salinity and density anomaly (sigma-*t*) at the observed Chl *a* maxima and the average stratification parameter on 22 July were close to the total average in the entire study period, while the maxima occurred clearly at deeper depths and lower temperatures than on average. The depth of occurrence of sub-surface Chl *a* maxima and corresponding water density increased from south to north. The maxima were constrained between the depths from 22.2 to 28.2 m and isopycnals from 4.80 to 5.22 kg m⁻³ in the northern part and at depths from 21.6 to 22.8 m and isopycnals from 4.82 to 4.94 kg m⁻³ in a relatively narrow region in the southern half of the section (Fig. 7C). The Chl *a* values in the sub-surface maxima also were the highest on 22 July—in a half of maxima the Chl *a* fluorescence signal was 6–10 times higher than the background level of 1–1.5 mg m⁻³. At the same time, the maximum Chl *a* values on the corresponding profiles in the surface layer were between 5.18 and 8.83 mg m⁻³ with an average of 7.30 mg m⁻³. Thus, the bimodal distribution was characterized by a thicker maximum with lower concentrations of Chl *a* in the upper layer and a thin maximum with very high Chl *a* concentrations in the deeper part of the thermocline.

Clear temporal trends in the analyzed parameters associated with the sub-surface Chl *a* maxima could not be detected, rather the observed variability was a result of dominating hydrodynamic forcing. After the most intensive appearance of the sub-surface maxima on 22 July, the next survey in the central part of the gulf on 26 July revealed only moderate maxima and associated bimodal vertical distribution of Chl *a*. As seen from the variations in the horizontal and vertical distributions of temperature and salinity (Figs. 2A, B and 3A, B), the upwelling event occurred near the southern coast and the upwelling waters reached the study site (buoy station) on 25 July. On 27 July, relatively intense sub-surface maxima were observed along the Scanfish section from the buoy station westwards (Fig. 8C). The most intense maxima were located in the area where the isopycnals, along which the maxima occurred, had the deepest position. On 30 July, the maxima were slightly less intense and occurred at slightly higher salinities and density anomalies than during the previous survey (Table 1). The last survey on 2 August detected only a few maxima near both the slopes. Due to the low salinity water mass, which occupied the surface layer in the study area in late July to early August (Figs. 2B and 3B), the stratification parameter was the highest and the maxima occurred at higher temperatures and lower salinities than before.

All described surveys were conducted during the daytime, except that on 20–21 July. Although the sub-surface maxima of Chl *a* were not observed at the buoy station at night, the bimodal distribution was recorded at 94 out of 246 profiles during the survey from 23:15 p.m. on 20 July to 06:15 a.m. on 21 July. The main difference with the other surveys was that, on average, the maxima were located at shallower depths and higher temperatures—at 17.8 m and 8.03 °C, respectively. On the Chl *a* fluorescence profiles, where the sub-surface maxima occurred, the bimodal distribution had a relatively thin local minimum between the broad upper layer maximum with moderate Chl *a* values and the sharp sub-surface maximum.

The bimodal vertical distribution of Chl *a* was mainly observed in those parts of each Scanfish section where the vertical stratification was weaker than along the rest of the section or at a local minimum of stratification. In order to demonstrate this link, the maxima and stratification in the upper 25 m layer were described quantitatively as outlined above. For the Scanfish sections, which were directed across the gulf (e.g., on 22 July, Fig. 9A), the connection between the stratification and occurrence of sub-surface maxima is well seen. The maxima were most intense in the part of the sections with the lowest values of the stratification parameter. In addition, a narrow region with the sub-surface maxima, which occurred on 22 July at distances of 22–24 km (Figs. 7C and 9A), coincided with a local minimum of the stratification parameter. On 27 July, the maxima did not occur in the part of the section with high values of stratification parameters (Fig. 9B) corresponding to the warm and less-saline side of the upwelling front. In the rest of the section, the vertical distribution of Chl *a* was mostly bimodal. However, at the lowest values of the stratification parameter the sub-surface maxima were absent or occurred with low intensities. Thus, the Chl *a* maxima did not occur in areas of the coastal upwelling event or its filaments, where the cold water has been surfaced (see Fig. 8A). The same was valid for the survey on 30 July that in turn resulted in a higher stratification parameter in the region with the sub-surface Chl *a* maxima than that at the rest of the section (Table 1).

A characteristic feature of the vertical Chl *a* distribution, which was also noticed at the sampling stations AP9–AP13 on 22 July, is related to the less pronounced local minimum between the surface and sub-surface Chl *a* maxima at some sites. The high-resolution profiling using the towed undulating vehicle has exposed that such a less-pronounced minimum appears in stretches with slightly higher Chl *a* concentrations in this intermediate water layer (in the water layer between the two maxima). These stretches with a horizontal scale of about 1–1.5 km could be detected at a few neighboring profiles on 22 July (Fig. 7C) and also during other surveys, e.g., on 27 July (Fig. 8C). Furthermore, a local maximum of Chl *a* was observed at about 25 of the northernmost profiles at the depths of the sharpest part of the thermocline (strongest vertical gradient of density) on

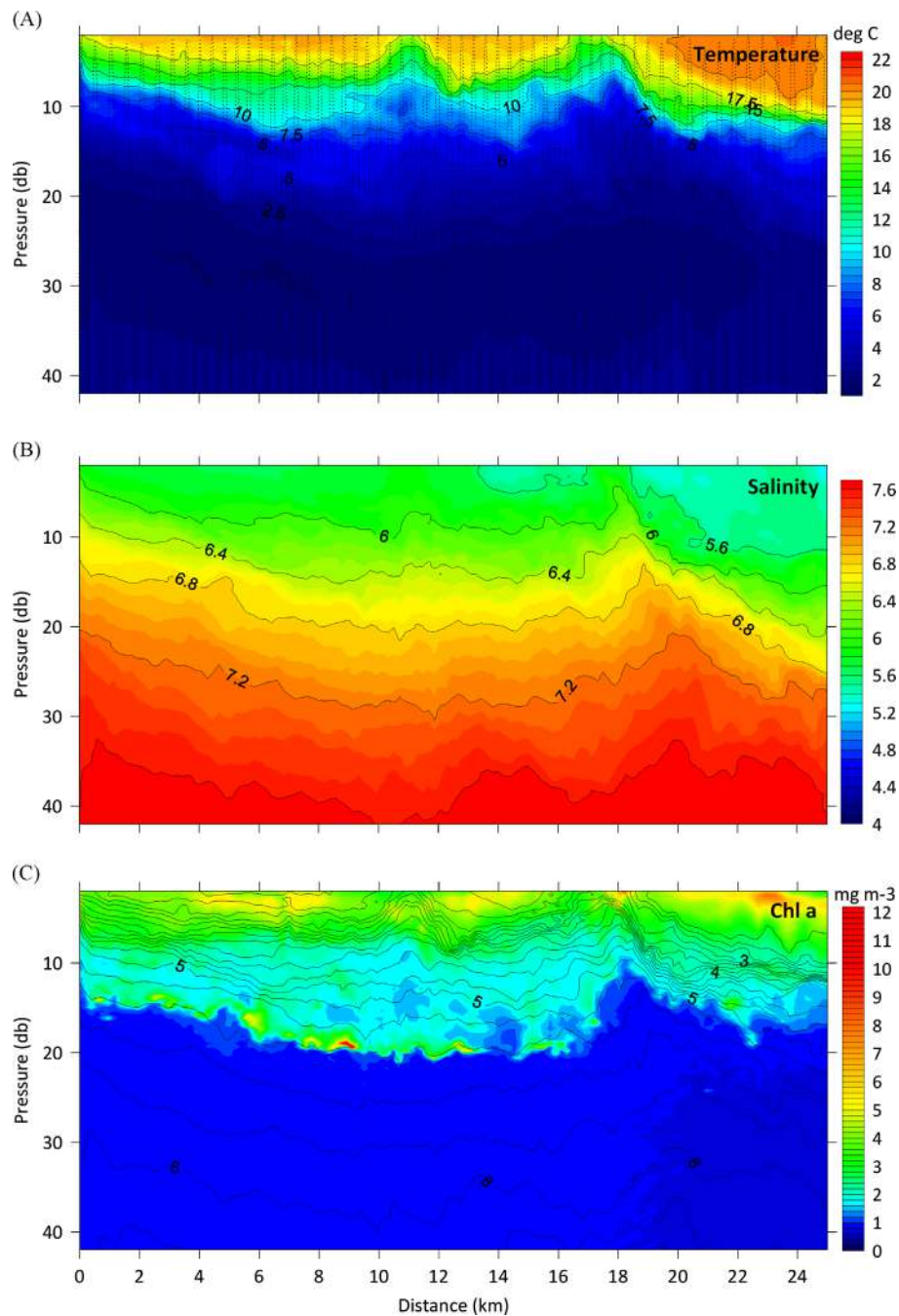


Fig. 8. Vertical sections of (A) temperature ($^{\circ}\text{C}$), (B) salinity, and (C) chlorophyll *a* (mg m^{-3} , color scale) and density anomaly (kg m^{-3} , black lines) measured by the towed undulating vehicle (Scanfish) on 27 July 2010. The Scanfish trajectory is shown in the upper panel as dotted lines. Distance on the x-axis is calculated from the westernmost profile.

22 July, which had an inclination opposite to that of the intense sub-surface maxima at the same set of profiles.

5. Discussion and conclusions

An extensive data set on vertical distributions of temperature, salinity, density anomaly, and Chl *a* fluorescence has been presented here for the Gulf of Finland in July 2010. In about one-third of the profiles recorded during six Scanfish surveys within 14 days in a relatively large area of the Gulf of Finland, bimodal vertical distribution of Chl *a* with a sub-surface maximum exceeding at least three times the background Chl *a* value was detected. In the

case of the bimodal distribution, the Chl *a* maximum in the upper 10 m layer was relatively thick while the sub-surface maximum in the deeper part of the thermocline was sharp corresponding to the thin layer definition (Dekshenieks et al., 2001). Temperature, salinity, and density values at the sub-surface Chl *a* maxima varied substantially between the surveys although they were not very variable during a single survey. It is concluded that the occurrence of sub-surface maxima and related thin layers was not linked to the presence of a certain water mass, in contrast to that found in the Northern Monterey Bay in July 2006 (Cheriton et al., 2010).

The measurements at the buoy station on 17–24 July clearly showed downward and upward migration of phytoplankton between the sea surface and upper part of the thermocline. The

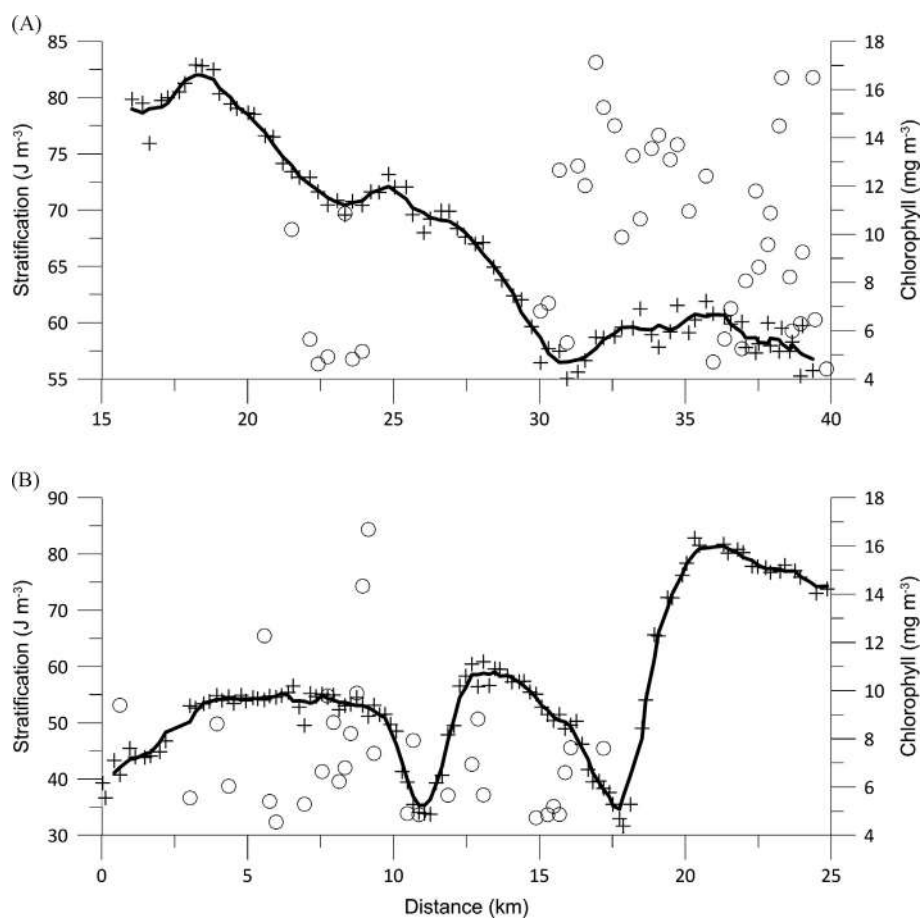


Fig. 9. Stratification parameter estimated in the layer 3–25 m on the basis of CTD profiles (crosses; the solid line represents the 5-point moving average) and maximum chlorophyll *a* value in the sub-surface maxima (open circles) measured by the towed undulating vehicle on 22 July 2010 (A) and 27 July 2010 and (B). Presented data correspond to the sections shown in Figs. 7 and 8.

formation of sub-surface Chl *a* maxima due to the downward migration of phytoplankton through the thermocline was also evident, but the upward migration of cells from below the strongest density gradient was not well documented at the same site. Based on the data of an earlier study (Lips et al., 2011), a suggestion has been made that part of the community could experience vertical migration with diel cycle, while part of it could stay below the thermocline for a longer period. Kononen et al. (2003) estimated that the dinoflagellate *H. triquetra* was able to survive below the thermocline for up to 6 days. All our measurements in the Gulf of Finland (Lips et al., 2010; Lips et al., 2011 and this study) have shown that the sub-surface maxima were located exactly at the depths of the nitracline. Thus, the formation of sub-surface Chl *a* maxima is triggered by the vertical migration of cells towards the deep nutrient reserves.

Physical processes (mechanisms) which, in combination with vertical migration, could play a role in formation of thin layers are straining by a sheared flow, intrusions, and gyrotactic trapping (Durham and Stocker, 2012). The observed tilt of the maxima, which were captured by a few consecutive Scanfish profiles in the northern part of the section on 22 July, can be judged as a sign of existing vertical shear at these depths. Such tilt of patches across surfaces of constant density has been suggested as a characteristic feature of thin layers formed by straining (Birch et al., 2008). Nevertheless, since the highest Chl *a* values were detected in the thinnest maxima layers, straining can be excluded as a single mechanism of thin layer formation in this particular study. Intrusions can also be excluded as a single mechanism of thin layer formation based on the same reasoning—such high chlorophyll

values were not observed elsewhere except in the thin layers. However, if considering targeted vertical migration of cells towards nutrient reserves, i.e., the nitracline, then both intrusions and vertical shear could contribute to the thin layer formation by thinning of patches of high Chl *a* content.

Since the sub-surface Chl *a* maxima were observed below the strongest density gradient, trapping of cells below it could be a mechanism of thin-layer formation. Similar occurrence of thin layers of Chl *a* maxima below the depth of the strongest stratification was observed by Johnston et al. (2009). The main arguments against such a trapping mechanism in our study are related to the observed stratification—the strongest vertical density gradient was about 10 m above the sub-surface Chl *a* maxima (Fig. 7C), and the maxima were most pronounced in the areas with weaker stratification if compared with the stratification at other sites during the same survey. Furthermore, almost all cells of *H. triquetra* in the samples collected from the sub-surface maxima were healthy, and settling down of cells from the maxima was not registered. The observational evidence that the Chl *a* fluorescence signal was almost absent below the sub-surface maxima (Figs. 3 and 6–8) is an additional argument to exclude convergent swimming or gyrotactic trapping (Durham and Stocker, 2012) as the mechanisms of thin-layer formation in our study.

We suggest that the areas and time periods where and when the vertical profiles of Chl *a* had bimodal distribution, but the local minimum between those maxima was not well pronounced, correspond to the areas and time periods where and when the upward migration of cells took place. At the northernmost CTD stations on 22 July, some thicker layers with Chl *a* concentration

exceeding 3–4 mg m⁻³ were evident above the sub-surface maxima (Fig. 6, stations AP9 and AP11). On the northern part of the Scanfish section on the same day (Fig. 7C), and also during other surveys (e.g., on 27 July, Fig. 8C), we noticed suc stretches with a slightly higher Chl *a* content as well. Since these features in the Chl *a* distribution were not restricted to the near-slope area, where more intense vertical mixing can be assumed (Reissmann et al., 2009), they may be connected to the vertical migration of cells. We assume that the migration in such stretches was directed upward since the measurements were made in daytime and we have not observed downward migration in daytime at the buoy station. This migration pattern is asynchronous if we consider the community in the entire study area, but at some locations a distinctive part of the community migrates between the two vertically separated biomass maxima in a synchronized way and creates the observed feature in the Chl *a* distribution.

The sub-surface maxima and previously mentioned stretches of slightly higher Chl *a* content were mostly limited to the areas where weaker stratification in the upper 25 m layer was observed at the mesoscale (from a few to 10 km, Figs. 7 and 9). Thus, a mesoscale anomaly of the stratification in space towards its weakening had to be present for the formation of intense sub-surface maxima. However, this conclusion is not an absolute statement—the maxima were almost absent below the upwelled waters on 27 and 30 July where the estimated stratification parameter clearly had the lowest values. In addition to the locally weaker stratification, circulation at the mesoscale might also be crucial for the formation of the bimodal Chl *a* distribution pattern. Most probably, the dynamics in these areas of weaker vertical stratification, which can be treated as anticyclonic eddies and/or filaments, work against the dispersion of cells or even support the phytoplankton accumulation in such features at the sub-surface depths. Concentration of migrating plankton, both in the surface and sub-surface layer, in response to the mesoscale variability, has been shown by several observational and modeling studies in the ocean environment (e.g., Mackas et al., 2005; Lima et al., 2002).

The observed increase in *H. triquetra* biomass in late July in the northern part of the ferry route points to the success of described migration patterns. Similar concurrent growth of *H. triquetra* biomass in the surface layer and appearance of sub-surface maxima were reported in the western part of the Gulf of Finland in July 1998 (Kononen et al., 2003) and in the present study area in July 2009 (Lips et al., 2011). In both mentioned cases as well as in July 2006 (Lips et al., 2010), the upwelling events were observed before or during the period of sub-surface Chl *a* maxima formation. The sub-surface maxima were also connected to the coastal upwelling events off Monterey Bay in 2003 (Johnston et al., 2009). Kononen et al. (2003) suggested that the sub-surface maxima in July 1998 were formed as a result of changing migratory behavior of *H. triquetra* after an upwelling event that fertilized the upper layer with phosphorus. However, high biomass values of *H. triquetra* in the surface layer and intense sub-surface Chl *a* maxima found in July 2006, disappeared almost completely after a very extensive upwelling event in early August (Lips and Lips, 2010). Analysis of temporal changes of vertical stratification and related processes revealed that in July–August 2009 the sub-surface maxima also disappeared when, after an upwelling event, a classical estuarine circulation scheme in low-wind conditions was re-established (Liblik and Lips, 2012). All these findings suggest that the vertical migration of *H. triquetra* and related formation of sub-surface biomass maxima is favored by relatively intense mesoscale dynamics, especially when off- and on-shore movements of waters at the opposite coasts occur. However, too intense forcing and upwelling events overrule this pattern.

We have noticed that the Chl *a* maxima were mostly found in the areas below the more saline surface layer along a particular

section, although low salinity waters were present occasionally in the upper part of the thermocline at the same sites (e.g., Fig. 7B). The latter suggests that the layered flow structure occurred in the thermocline when the sub-surface maxima were observed in the deeper part of it. Thus, we suggest that the sub-mesoscale intrusions along inclined surfaces of constant density in cases of relatively high mesoscale activity could play a role in sub-surface Chl *a* maxima formation.

The main species found in the sub-surface Chl *a* maxima in the deeper part of the thermocline in the Gulf of Finland has been the dinoflagellate *H. triquetra* (Lips et al., 2011; Kononen et al., 2003). In addition to this species, in our samples collected in July 2010, *D. acuminata* was also occasionally present in high biomass. Since the light levels at the thermocline usually do not support efficient autotrophic growth of *Dinophysis* spp. (Carpenter et al., 1995), they would need to migrate to higher light levels. It has been shown that *D. acuminata* performs phototactic vertical migrations in some environments (Figueroa et al., 1998; Villarino et al., 1995), mainly between the surface layer and 10 m depth. In the Baltic Sea, including the Gulf of Finland, the higher abundances of *D. acuminata* have been detected also mostly in the upper 15 m mixed layer (Hällfors et al., 2011) except one record of *D. acuminata* population below the highest density gradient in the Baltic Proper (Setälä et al., 2005). During our studies in 2010, the cells of *D. acuminata* were mostly distributed in the upper layer between the depths of 5 and 15 m (Fig. 5). In late July, the high cell abundances were detected also clearly below the highest density gradient at the 20 m depth just above the nitracline (Figs. 5d and 6). The abundances in this layer were measured on 22 July as > 10 000 cells l⁻¹ and 5500 cells l⁻¹ at stations AP5 and AP7, respectively.

There might exist two different populations of *D. acuminata*: the population found in the upper mixed layer could be able to perform phototactic diel vertical migrations in order to feed on dissolved or particulate organic matter at night and photosynthesize during light periods. The population below the pycnocline could depend merely on phagotrophy. This suggestion is supported by findings of Setälä et al. (2005) who studied the *D. acuminata* population sampled at 70–80 m depth where the photosynthetic rates of populations were low, even though the cells still contained chloroplasts, suggesting that the cells were adapted to phagotrophic nutrition.

The preference of mixotrophic organisms to concentrate on deeper layers of the water column might also be associated with the presence of specific prey. The vacuolated cells of *D. acuminata* have often been found with the presence of ciliate *M. rubra* in the community (e.g., Velo-Suarez et al., 2008). During recent years, several studies have shown evidence of *D. acuminata* feeding on *M. rubra* (García-Cuetos et al., 2010; Riisgaard and Hansen, 2009). On the basis of data for 22 July, the biomass of *M. rubra* seemed in our study area to be controlled by *D. acuminata* in the illuminated upper mixed layer (Fig. 6), except at the northernmost stations.

In conclusion, there are two main consequences of the described vertical dynamics and bimodal distribution pattern of phytoplankton in the stratified Gulf of Finland. First, the occurrence of sub-surface Chl *a* maxima shows that the flagellated phytoplankton is able to utilize the deep reserves of nitrate through undergoing a migration cycle with a longer period than a day. This migration pattern is successful with a higher probability in the case of relatively high horizontal variability of vertical stratification at the mesoscale in areas with weaker stratification. We suggest that besides the upwelling events and vertical turbulent mixing, the selective utilization of nutrients at sub-surface depths and vertical migration of cells under favorable conditions could significantly contribute to the transport of nutrients in a stratified estuary.

Secondly, the layered structure of phytoplankton distribution and associated migration patterns depend on the dominating

species and their survival strategies. Diel migration down to the upper part of the thermocline at night and back to the sea surface in the morning has been demonstrated. It can be related to the species' (e.g., *D. acuminata*) ability to utilize organic nitrogen compounds at the strongest vertical density gradient in the upper part of the thermocline. Regarding *H. triquetra*, we assume that this species experiences vertical migration with a longer period than 24 h. If hydrodynamic processes favor this migration pattern of *H. triquetra* then it can form surface blooms in a background of limiting inorganic nutrients. Thus, in order to secure the continuous assessment of the state of the marine environment and short-term forecasts of phytoplankton blooms, layered vertical distribution of phytoplankton including sub-surface biomass maxima need to be described in the operational systems.

Acknowledgments

The work was partly financed by the Estonian Science Foundation (research grants ETF6955, ETF8930 and ETF9023). We thank our colleagues and students Villu Kikas, Taavi Liblik, Aet Meerits, Nelli Rünk, and Andres Trei for their assistance in conducting the observations, sample analyses, and data processing.

References

- Alenius, P., Myrberg, K., Nekrasov, A., 1998. The physical oceanography of the Gulf of Finland: a review. *Boreal Environ. Res.* 3, 97–125.
- Ammerman, J., 2001. QuikChem[®] Method 31-115-01-1-1—Determination of orthophosphate by flow injection analysis. Lachat Instruments.
- Birch, D.A., Young, W.R., Franks, P.J.S., 2008. Thin layers of plankton: formation by shear and death by diffusion. *Deep-Sea Res.* 55, 277–295.
- Carpenter, E.J., Jansson, S., Boje, R., Pollehne, F., Chang, J., 1995. The dinoflagellate *Dinophysis norvegica*: biological and ecological observations in the Baltic Sea. *Eur. J. Phycol.* 30, 1–9.
- Cheriton, O.M., McManus, M.A., Steinbeck, J.V., Stacey, M.T., Sullivan, J.M., 2010. Towed vehicle observations of thin layer structure and low-salinity intrusion in Northern Monterey Bay, CA. *Cont. Shelf Res.* 30, 39–49.
- Dekshenieks, M.M., Donaghay, P.L., Sullivan, J.M., Rines, J.E.B., Osborn, T.R., Twardowski, M.S., 2001. Temporal and spatial occurrence of thin phytoplankton layers in relation to physical processes. *Mar. Ecol. Prog. Ser.* 223, 61–71.
- Durham, W.M., Stocker, R., 2012. Thin phytoplankton layers: characteristics, mechanisms, and consequences. *Annual Rev. Mar. Sci.* 4, 177–207.
- Egan, L., 2000. QuikChem[®] Method 31-107-04-1-D—Determination of nitrate and/or nitrite in brackish waters by flow injection analysis. Lachat Instruments.
- Figuerola, F.L., Niell, F.X., Figueiras, F.G., Villarino, M.L., 1998. Diel migration of phytoplankton and spectral light field in the Ria de Vigo (NW Spain). *Mar. Biol.* 130, 491–499.
- García-Cuetos, L., Moestrup, O., Hansen, P.J., Daugbjerg, N., 2010. The toxic dinoflagellate *Dinophysis acuminata* harbors permanent chloroplasts of cryptomonad origin, not kleptochloroplasts. *Harmful Algae* 9, 25–38.
- Gisselso, G.-Å., Carlsson, P., Graneli, E., Pallon, J., 2002. *Dynophysis* bloom in the deep euphotic zone of the Baltic Sea: do they grow in the dark? *Harmful Algae* 1, 401–418.
- Hall, N.S., Paerl, H.W., 2011. Vertical migration patterns of phytoflagellates in relation to light and nutrient availability in shallow microtidal estuary. *Mar. Ecol. Prog. Ser.* 425, 1–19.
- Hällfors, H., Hajdu, S., Kuosa, H., Larsson, U., 2011. Vertical and temporal distribution of the dinoflagellates *Dinophysis acuminata* and *D. norvegica* in the Baltic Sea. *Boreal Environ. Res.* 16, 121–135.
- HELCOM, 1988. Guidelines for the Baltic monitoring programme for the third stage. Part D. Biological determinants. *Baltic Sea Environ. Proc.* 27D, 1–161.
- Jephson, T., Fagerberg, T., Carlsson, P., 2011. Dependency of dinoflagellates vertical migration on salinity stratification. *Aquat. Microb. Ecol.* 63, 255–264.
- Johnston, T.M.S., Cheriton, O.M., Pennington, J.T., Chavez, F.P., 2009. Thin phytoplankton layer formation at eddies, filaments, and fronts in a coastal upwelling zone. *Deep-Sea Res.* II 56, 246–259.
- Kahru, M., Savchuk, O.P., Elmgren, R., 2007. Satellite measurements of cyanobacterial bloom frequency in the Baltic Sea: interannual and spatial variability. *Mar. Ecol. Prog. Ser.* 343, 15–23.
- Kononen, K., Huttunen, M., Hällfors, S., Gentien, P., Lunven, M., Huttula, T., Laanemets, J., Lilover, M.-J., Pavelson, J., Stips, A., 2003. Development of a deep chlorophyll maximum of *Heterocapsa triquetra* Ehrenb. at the entrance to the Gulf of Finland. *Limnol. Oceanogr.* 48, 594–607.
- Kononen, K., Kuparinen, J., Mäkelä, K., Laanemets, J., Pavelson, J., Nömmann, S., 1996. Initiation of cyanobacterial blooms in a frontal region at the entrance of the Gulf of Finland, Baltic Sea. *Limnol. Oceanogr.* 41, 98–112.
- Laanemets, J., Väli, G., Zhurbas, V., Elken, J., Lips, I., Lips, U., 2011. Simulation of mesoscale structures and nutrient transport during summer upwelling events in the Gulf of Finland in 2006. *Boreal Environ. Res.* 16A, 15–26.
- Liblik, T., Lips, U., 2012. Variability of synoptic-scale quasi-stationary thermohaline stratification patterns in the Gulf of Finland in summer 2009. *Ocean Sci.* 8, 603–614.
- Lima, I.D., Olson, D.B., Doney, S.D., 2002. Biological response to frontal dynamics and mesoscale variability in oligotrophic environments: biological production and community structure. *J. Geophys. Res. Oceans* 107, C83111, <http://dx.doi.org/10.1029/2000jc000393>.
- Lindholm, T., Nummelin, C., 1999. Red tide of the dinoflagellates *Heterocapsa triquetra* (Dinophyta) in a ferry-mixed coastal inlet. *Hydrobiologia* 393, 245–251.
- Lips, I., Lips, U., 2010. Phytoplankton dynamics affected by the coastal upwelling events in the Gulf of Finland in July–August 2006. *J. Plankton Res.* 32, 1269–1282.
- Lips, U., Lips, I., Liblik, T., Kikas, V., Altoja, K., Buhhalko, N., Rünk, N., 2011. Vertical dynamics of summer phytoplankton in a stratified estuary (Gulf of Finland, Baltic Sea). *Ocean Dyn.* 61, 903–915.
- Lips, U., Lips, I., Liblik, T., Kuvaldina, N., 2010. Processes responsible for the formation and maintenance of sub-surface chlorophyll maxima in the Gulf of Finland. *Estuar. Coast. Shelf Sci.* 88, 339–349.
- Mackas, D., Tsurumi, M., Galbraith, M., Yelland, D., 2005. Zooplankton distribution and dynamics in a North Pacific Eddy of coastal origin: II. Mechanisms of eddy colonization by and retention of offshore species. *Deep-Sea Res.* II 57, 1011–1036.
- Olenina, I., Hajdu, S., Edler, L., Andersson, A., Wasmund, N., Busch, S., Göbel, J., Gromisz, S., Huseby, S., Huttunen, M., Jaanus, A., Kokkonen, P., Ledaine, I., Niemkiewicz, E., 2006. Biovolumes and size-classes of phytoplankton in the Baltic Sea. *HELCOM Baltic Sea Environ. Proc.* 106, 144.
- Ralston, D.K., McGillicuddy, D.J., Townsend, D.W., 2007. Asynchronous vertical migration and bimodal distribution of motile phytoplankton. *J. Plankton Res.* 29, 803–821.
- Reissmann, J.H., Burchard, H., Feistel, R., Hagen, E., Lass, H.U., Mohrholz, V., Nausch, G., Umlauf, L., Wiczorek, G., 2009. Vertical mixing in the Baltic Sea and consequences for eutrophication—a review. *Prog. Oceanogr.* 82, 47–80.
- Riisgaard, K., Hansen, P.J., 2009. Role of food uptake for photosynthesis, growth and survival of the mixotrophic dinoflagellate *Dinophysis acuminata*. *Mar. Ecol. Prog. Ser.* 381, 51–62.
- Setälä, O., Sopanen, S., Autio, R., Kankaanpää, H., Erler, K., 2011. Dinoflagellate toxins in the northern Baltic Sea phytoplankton and zooplankton assemblages. *Boreal Environ. Res.* 16, 509–520.
- Setälä, O., Autio, R., Kuosa, H., Rintala, J., Ylöstalo, P., 2005. Survival and photosynthetic activity of different *Dinophysis acuminata* populations in the northern Baltic Sea. *Harmful Algae* 2, 337–350.
- Simpson, J.H., Brown, J., Matthews, J., Allen, G., 1990. Tidal straining, density currents, and stirring in the control of estuarine stratification. *Estuaries* 13, 125–132.
- Sullivan, J.M., Donaghay, P.L., Rines, J.E.B., 2010. Coastal thin layer dynamics: consequences to biology and optics. *Cont. Shelf Res.* 30, 50–65.
- Townsend, D.W., Bennet, S.L., Thomas, M.A., 2005. Diel vertical distributions of the red tide dinoflagellate *Alexandrium fundyense* in the Gulf of Maine. *Deep-Sea Res.* II 52, 2593–2602.
- Utermöhl, H., 1958. Zur Vervollkommnung der quantitativen Phytoplanktonmetodik. *Mitteilungen des Internationale Vereinigung für Theoretische und Angewandte Limnologie* 9, 1–38.
- Velo-Suarez, L., Fernand, M., Gentien, P., Reguera, B., 2010. Hydrodynamic conditions associated with the formation, maintenance and dissipation of a phytoplankton thin layer in a coastal upwelling system. *Cont. Shelf Res.* 30, 193–202.
- Velo-Suarez, L., Gonzales-Gil, S., Gentien, P., Lunven, M., Bechemin, C., Fernand, L., Raine, R., Reguera, B., 2008. Thin layers of *Pseudo-nitzschia* spp. and the fate of *Dynophysis acuminata* during an upwelling-downwelling cycle in a Galician Ria. *Limnol. Oceanogr.* 53, 1816–1834.
- Villarino, M.L., Figueiras, F.G., Jones, K.J., Alvarez-Salgado, X.A., Richard, J., Edwards, A., 1995. Evidence of *in situ* diel vertical migration of a red-tide microplankton species in Ria de Vigo (NW Spain). *Mar. Biol.* 123, 607–617.